Fast macroscopic-superposition-state generation by coherent driving

Emi Yukawa,[1,2,*] G. J. Milburn,[3] and Kae Nemoto[1]

[1] *National Institute of Informatics, 2-1-2 Hitotsubashi, Chiyoda-ku, Tokyo 101-8430, Japan*
[2] *RIKEN Center for Emergent Matter Science, 2-1, Hirosawa, Wako-shi, Saitama, 351-0198, Japan*
[3] *Centre for Engineered Quantum Systems, School of Mathematics and Physics, The University of Queensland, St Lucia, QLD 4072, Australia*

(Dated: March 17, 2017)

We propose a scheme to generate macroscopic superposition states in spin ensembles, where a coherent driving field is applied to accelerate the generation of macroscopic superposition states. The numerical calculation demonstrates that this approach allows us to generate a superposition of two classically distinct states of the spin ensemble with a high fidelity above 0.96 for 300 spins. For the larger spin ensemble, though the fidelity slightly decline, it maintains above 0.85 for an ensemble of 500 spins. The time to generate a macroscopic superposition state is also numerically calculated, which shows that the significantly shortened generation time allows us to achieve such macroscopic superposition states within a typical coherent time of the system.

arXiv:1703.05666v1 [quant-ph] 16 Mar 2017

For a long time quantum mechanics has been considered as the theory to describe physical behaviour in the microscopic scale, and the quantum theory has provided the framework for the development of the technologies, which clearly characterise the twenties century. Semiconductor-based computer technology and laser are typical examples which require quantum-mechanical understanding in the underlying physics. Our effort to manipulate quantum coherence did not however stop there, and in the recent years it continued to realize a longer coherence time and a higher fidelity. As one of the consequences of this development, we began to manipulate quantum coherence in macroscopic states of matter [1].

To further penetrate this new quantum regime, it is necessary, however, to circumvent experimental obstacles for a system to behave quantum mechanically in an even large scale. For instance, the non-classical generation of states, such as squeezed states [2] and the $N00N$ states [3], has its limitation in reality: squeezing becomes too noisy when squeezing gets too large, and the success probability or the fidelity of noon states is plummeted when n gets larger. Superposition states of two or several coherent states progressively become difficult to generate as the coherent states approach to be orthogonal. These non-classical states are not only interesting as a promising candidate for quantum technology such as high precision measurements, but the macroscopic non-classical states are also a route to novel quantum phenomena never achievable before. To realise these states, as the attainable precision has its own limitation even with the best technology, it is essential to introduce a new mechanism for quantum properties to win over its decoherence. In this Letter, we focus on collective spin systems and show how such macroscopic non-classical states can be generated.

* emi.yukawa@riken.jp

Collective spin states have been investigated in cold atom systems such as Bose-Einstein condensation and solid-state systems, where spins are abundant and its inhomogenious broadening is well suppressed. When a state form a superposition of two or more macroscopically distinguishable states, such as large coherent states, it is called macroscopic superposition states (MSSs) [9]. They are also known as N-particle Greenberger-Horne-Zeilinger (GHZ) states [7, 8], $N00N$ states [3], or macroscopic quantum superposition states [4–6], depending on what macroscopic nature we are interested in. These states are not only interesting for their macroscopic quantum behaviour, but they are also potentially applicable to Heisenberg-limited spectroscopy [8, 10–17], quantum computations with coherent states [18–20], and quantum repeaters [21], as we see them playing the central role in the implementation of quantum technology. Our primary interest in this Letter is a superposition state of two macroscopically distinguishable spin coherent state [22], which we refer as a spin cat state.

In an ensemble of N identical 1/2-spins, a spin cat state can be generated from a separable coherent spin state [22] via a number of ways. A quadratic interaction between spins [4–6, 15, 17, 23, 24, 26–29], the QND interaction [30, 31], and the dispersive Tavis-Cummings interaction [32, 33] generate these spin cat states, whereas a series of controlled-NOT gates [10, 16, 34], or a sequence of spin measurements [35–37] have been proposed. The quadratic interaction, essentially equivalent to the sequence of the controlled-NOT gates [39, 40], shows better scalability with respect to the number of spins. This interaction is often called the one-axis twisting interaction and is given by

$$\hat{H}_{\rm OAT} = \hbar\chi \hat{J}_z^2, \tag{1}$$

where χ represents the interaction energy and the collective spin operator is defined as $\hat{J}_\mu \equiv \frac{1}{2}\sum_{j=1}^{N} \hat{\sigma}_\mu^{(j)}$ ($\mu = x, y, z$) with the Pauli operator $\hat{\sigma}_\mu^{(j)}$ of the jth spin [41].

The Hamiltonian in Eq. (1) has been implemented in ultracold ^{87}Rb atomic gases with $N \sim \mathcal{O}(10^{2-4})$ spins to create squeezed spin states [42–45].

Spin cat states have been experimentally created in two-level systems of trapped ions [46], high-symmetry molecules in NMR [16], and circularly polarized light [34]. These cat stats are comprised of 4-14 spins and do not scale up to larger spin ensembles. One of the main factors is that the cat-state preparation via the one-axis twisting interaction in Eq. (1) requires an evolution time of $t = \pi/2\chi$ [4–6, 15, 23, 24, 28] which is comparable to at best or longer than the coherence time of the spin ensemble [42–45, 48] for the number of spins larger than $N \sim \mathcal{O}(10^2)$. To create a macroscopic spin cat state, one has to maintain its coherence beyond this interaction time, which remains challenging.

One strategy to shorten the evolution time to create the cat state is to utilize the transverse magnetic field [49–51]:

$$\hat{H}_{\rm LMG} = \hbar(\chi \hat{J}_z^2 + \Omega \hat{J}_x), \tag{2}$$

known as the Lipkin-Meshkov-Glick Hamiltonian [52] and implemented in a cold-atomic system to generate squeezed spin states [45]. Not only squeezed spin states but spin cat states can be expected to be created via the Hamiltonian in Eq. (2) within the evolution time of $t \sim \mathcal{O}(\log N/\chi N)$; however, the fidelity to the cat state degrades as the number of spins increases to be $\sim \mathcal{O}(10^2)$ [51].

We here propose a scheme to apply a coherent driving field to the spin ensemble in order to speed up the cat-state creation via Eq. (1). We numerically demonstrate that this scheme can generate a macroscopic superposition state with the fidelity to the ideal cat state above 0.85 for the number of spins up to 500. The time scale to generate a cat state can be made shorter than or comparable to coherence times of atomic gases.

We consider a collective spin system consisting of N identical 1/2 spins with two degrees of freedom $|\uparrow\rangle$ and $|\downarrow\rangle$. A single-spin state can be parametrized as $|\alpha,\beta\rangle \equiv \cos\frac{\beta}{2}|\uparrow\rangle + e^{i\alpha}\sin\frac{\beta}{2}|\downarrow\rangle$ by a set of the polar and azimuth angles (α,β) ($\alpha \in (-\pi,\pi]$ and $\beta \in [0,\pi]$). A coherent spin state of the N-spin ensemble can also be expressed in terms of α and β as

$$\begin{aligned}|\Psi_{\rm CSS}(J;\alpha,\beta)\rangle &= |\alpha,\beta\rangle^{\otimes 2J} \\ &= \sum_{n=0}^{2J} \sqrt{{}_{2J}{\rm C}_n}\, \cos^{2J-n}\left(\frac{\beta}{2}\right)\, \sin^n\left(\frac{\beta}{2}\right)\, e^{in\alpha}|J, J-n\rangle,\end{aligned} \tag{3}$$

where $J = N/2$ represents the total spin and $|J,M\rangle$ denotes the eigenstate of the collective spin operator $\hat{J}_z$ corresponding to the eigenvalue M. Setting $|\Psi_{\rm CSS}(J;0,\frac{\pi}{2})\rangle$ as the initial state, we consider the time evolution by the Hamiltonian composed of the one-axis twisting Hamiltonian in Eq. (1) and the coherent driving field,

$$\hat{H}(J;t) = \hbar[\chi \hat{J}_z^2 + \Omega \hat{J}_x \cos(\omega_{\rm drv} t + \phi_{\rm drv})], \tag{4}$$

where Ω, $\omega_{\rm drv}$, and $\phi_{\rm drv}$ denote the driving energy, the driving frequency, and the phase of the driving field, respectively. Here, we define $\lambda \equiv 2\chi J$ and rescale the elapsed time, the driving energy, and the driving frequency as $\tau \equiv \lambda t$, $r \equiv \Omega/\lambda$, and $\tilde{\omega}_{\rm drv} \equiv \omega_{\rm drv}/\lambda$. Throughout the paper, r is fixed at $r = 1$, while J, $\omega_{\rm drv}$, and $\phi_{\rm drv}$ are left to be tunable. Under the Hamiltonian (4), the initial state evolves as $|\Psi(J;\tau)\rangle \equiv \exp[\tilde{H}\tau/i\hbar]|\Psi_{\rm CSS}(J;0,\pi/2)\rangle$, where $\tilde{H} \equiv \hbar[(2J)^{-1}\hat{J}_z^2 + \hat{J}_x\cos(\tilde{\omega}_{\rm drv}\tau + \phi_{\rm drv})]$. When $\tilde{\omega}_{\rm drv}$ is moderately slow and $\phi_{\rm drv} \simeq 0$, we can intuitively expect the initial x-polarized coherent spin state to become a superposition of two coherent spin states. This is because the mean-field stability analysis of the LMG Hamiltonian in Eq. (2) implies that the x-polarized state, i.e., the classical limit of the initial state, is the highest energy state for $r = 1$ and two states polarized to $(r, 0, \pm\sqrt{1-r^2})^T$ are the highest energy states for $r < 1$; hence the cosine-shape driving $\cos(\tilde{\omega}_{\rm drv}\tau)$ would smoothly bring the initial state to the superposition of the coherent spin states pointing in $(\cos(\tilde{\omega}_{\rm drv}\tau_{\rm fin}), 0, \pm\sqrt{1-\cos^2(\tilde{\omega}_{\rm drv}\tau_{\rm fin})})^T$ at $\tau = \tau_{\rm fin} > 0$.

The time evolution of the Q function for the state $|\Psi(J;\tau)\rangle$ is illustrated in the snapshots in Figs. 1, which indicates that the state $|\Psi(J;\tau)\rangle$ achieves a high fidelity to an MSS at (d) $\tau = 12$ and at (e) $\tau = 16$. An MSS can be parametrized in terms of three parameters α, β, and γ as in Ref. [6]:

$$\begin{aligned}&|\Psi_{\rm MSS}(J;\alpha,\beta,\gamma)\rangle \\ \equiv &\frac{|\Psi_{\rm CSS}(J;\alpha,\beta)\rangle + e^{i\gamma}|\Psi_{\rm CSS}(J;-\alpha,\pi-\beta)\rangle}{\sqrt{2[1+\cos(2J\alpha-\gamma)\,\cos^{2J}\alpha\,\sin^{2J}\beta]}},\end{aligned} \tag{5}$$

where $\alpha \in (-\pi,\pi]$, $\beta \in [0,\pi/2]$, $\gamma \in (-\pi,\pi]$, and $(\alpha,\beta,\gamma) \neq (0,\frac{\pi}{2},\gamma)$, $(\pi,\frac{\pi}{2},\gamma)$. The displacement angle δ between two superposed coherent spin states can be expressed in terms of α and β as $\delta(\alpha,\beta) = 2\arccos(\cos\alpha\sin\beta)$. The fidelity of the state $|\Psi(J;\tau)\rangle$ to the MSS in Eq. (5) is obtained by

$$F(J;t;\alpha,\beta,\gamma) \equiv |\langle\Psi_{\rm MSS}(J;\alpha,\beta,\gamma)|\Psi(J;t)\rangle|^2. \tag{6}$$

We optimize the fidelity in Eq. (6) with respect to the set (α,β,γ) in Eq. (5) via the basin-hopping method [55] and define

$$F_{\rm opt}(J;\tau) \equiv \max_{\alpha,\beta,\gamma} F(J;\tau;\alpha,\beta,\gamma), \tag{7}$$

$$\begin{aligned}&(\alpha_{\rm opt}(J;\tau),\beta_{\rm opt}(J;\tau),\gamma_{\rm opt}(J;\tau)) \\ &\qquad \equiv \arg\max_{\alpha,\beta,\gamma} F(J;\tau;\alpha,\beta,\gamma),\end{aligned} \tag{8}$$

$$\delta_{\rm opt}(J;\tau) \equiv \delta(\alpha_{\rm opt}(J;\tau),\beta_{\rm opt}(J;\tau)). \tag{9}$$

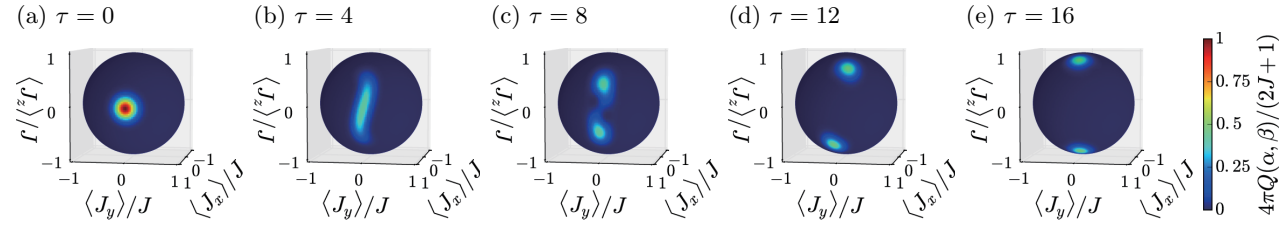

FIG. 1. (Color Online) Time evolution of the Q functions $Q(\alpha, \beta) \equiv \frac{2J+1}{4\pi} |\langle \Psi_{\rm CSS}(J; \alpha, \beta) | \Psi(J; \tau) \rangle|^2$ for $J = 50$, $\tilde{\omega}_{\rm drv} = 0.0204\pi$, and $\phi_{\rm drv} = 0.024\pi$ at the rescaled elapsed times of (a) $\tau = 0$, (b) 4, (c) 8, (d) 12, and (d) 16. The color at the point indicated by the polar and azimuthal angles of (α, β) represents $\frac{4\pi}{2J+1} Q(\alpha, \beta)$ according to the right gauge.

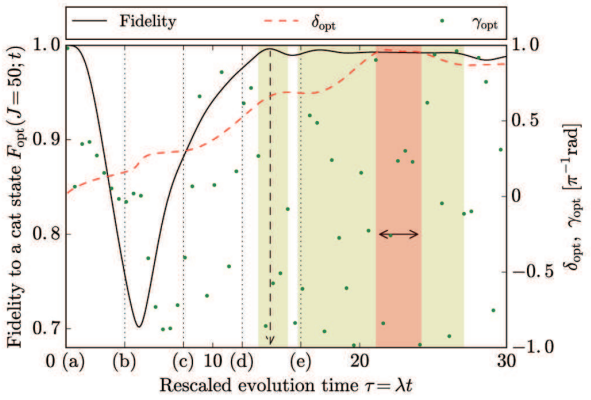
Fidelity
$\delta_{\rm opt}$
$\gamma_{\rm opt}$
Fidelity to a cat state $F_{\rm opt}(J=50;t)$
$\delta_{\rm opt}$, $\gamma_{\rm opt}$ $[\pi^{-1}{\rm rad}]$
Rescaled evolution time $\tau = \lambda t$

FIG. 2. (Color Online) Time dependences of the optimized fidelity $F_{\rm opt}(J; \tau)$, displacement angle $\delta_{\rm opt}(J; \tau)$, and phase $\gamma_{\rm opt}(J; t)$ for $J = 50$, $\tilde{\omega}_{\rm drv} = 0.0204\pi$, and $\phi_{\rm drv} = 0.0240\pi$. The solid curve with the left scale indicates $F_{\rm opt}(J; \tau)$. The red dotted line and the green dots with the right scale represent $\delta_{\rm opt}(J; \tau)$ and $\gamma_{\rm opt}(J; \tau)$, respectively. The rescaled evolution times corresponding to the snapshots (a)-(e) in Figs. 1 are indicated by the black dotted lines. The yellow shaded regions $13.1 \leq \tau \leq 15.1$ and $15.8 \leq \tau \leq 27.1$ has the fidelity exceeding 0.99. The red shaded region with a twin-headed arrow $21.1 \leq \tau \leq 24.2$ shows the fidelity larger than 0.99 and a large displacement angle $\delta_{\rm opt} \geq 0.95\pi$. The phase $\gamma_{\rm opt}(J; \tau)$ evolve very fast so that it seems to be random at a glance when we restrict $-\pi < \gamma_{\rm opt}(J; \tau) \leq \pi$ and use the identities $F(J; \tau; \alpha, \beta, \gamma) = F(J; \tau; \alpha, \beta, \gamma + 2n\pi)$ $(n \in \mathbb{Z})$ and $F(J; \tau; \alpha, \beta, \gamma) = F(J; \tau; \alpha, \beta, \gamma - 2J\alpha)$. The black dashed-dotted arrow indicates the first local maximum of the fidelity at $\tau = 13.9$.

The optimized fidelity in Eq. (7) has local maxima with respect to the rescaled evolution time τ. Taking $J = 50$, $\tilde{\omega}_{\rm drv} = 0.0204\pi$, and $\phi_{\rm drv} = 0.0240\pi$, as an example, we plot $F_{\rm opt}(J; \tau)$, $\delta_{\rm opt}(J; \tau)$, and $\gamma_{\rm opt}(J; \tau)$ in Fig. 2. Figure 2 indicates that the state $|\Psi(J; \tau)\rangle$ achieves an fidelity exceeding 0.99 at $\tau = 13.1$. After this optimal point, the state maintains high fidelity for quite a while, which implies that the fidelity is rather insensitive to timing in creating an MSS via this method. For the rescaled evolution time $21.1 \leq \tau \leq 24.2$, the displacement angle of the state $|\Psi(J; \tau)\rangle$ achieves $0.95\pi \geq \delta_{\rm opt} \leq \pi$; hence $|\Psi(J; \tau)\rangle$ is nearly SU(2) equivalent to $(|J, J\rangle + e^{i\gamma}|J, -J\rangle)/\sqrt{2}$.

Next, in order to investigate the driving frequency and its phase to optimise the fidelity, the displacement angle, and the evolution time, we define the rescaled evolution time $\tau_{\rm MSS}$ corresponding to the first local maximum of the fidelity (for instance, $\tau = 13.9$ in Fig. 2). We numerically obtain $\tau_{\rm MSS}$ and the corresponding fidelity $F_{\rm opt}(J; \tau_{\rm MSS}) \equiv F_{\rm MSS}(J)$ and displacement angle $\delta_{\rm opt}(J; \tau_{\rm MSS}) \equiv \delta_{\rm MSS}(J)$ for $J = 50$, 74.5, 100, 124.5, 150, 174.5, 200, and 250. The fidelity $F_{\rm MSS}(J)$ and the displacement angle $\delta_{\rm MSS}(J)$ are plotted in Figs. 3 for $J = 50$, 124.5, 174.5, and 250. For $J = 50$ in Fig. 3 (a), there is a region with high fidelity $F_{\rm MSS}(J) \sim 1$ and finite displacement angle $\delta_{\rm MSS}(J) \geq 0.5\pi$. For $J = 124.5$ in Fig. 3 (b), two regions shows high fidelity and large displacement angle. The left region in the figure shows higher fidelity than the right region. However, this left region of high fidelity disappears in Figs. 3 (c) and (d) for $J = 174.5$ and $J = 250$ respectively. This behaviour can even more clearly seen in the spin number dependency on the maximum fidelity as shown in Figs. 4. The maximum fidelity jumps in the regime $150 \leq J \leq 174.5$. Interestingly, this behaviour can be qualitatively explained with the Q function of $|\Psi(J; \tau)\rangle$ and the mean-field stability analysis. The two superposed states in $|\Psi(J; \tau_{\rm MSS})\rangle$ sit in the mean-field equal energy contour of $E = 2\hbar\lambda \cos(\tilde{\omega}_{\rm drv}\tau + \phi_{\rm drv})$ nearby the two centers $E = \hbar\lambda(1 + \cos^2(\tilde{\omega}_{\rm drv}\tau + \phi_{\rm drv}))$. For the parameter region with the higher fidelity, the Q function of $|\Psi(J; \tau)\rangle$ is almost distributed inside of the equal energy contour $E = 2\hbar\lambda \cos(\tilde{\omega}_{\rm drv}\tau + \phi_{\rm drv})$ at the early stage of the time evolution, while for the parameter region with the lower fidelity, the Q function of $|\Psi(J; \tau)\rangle$ at the early stage of the time evolution leaks from the equal energy contour due to the driving frequency higher than the high-fidelity parameter region. The population leaked from the equal-energy contour cannot cross the equal-energy contour back to its inside region, and hence it causes a decrease in the fidelity. This implies that there is no parameter region of $\tilde{\omega}_{\rm drv}$ and $\phi_{\rm drv}$ such that the Q function is efficiently confined in the equal-energy

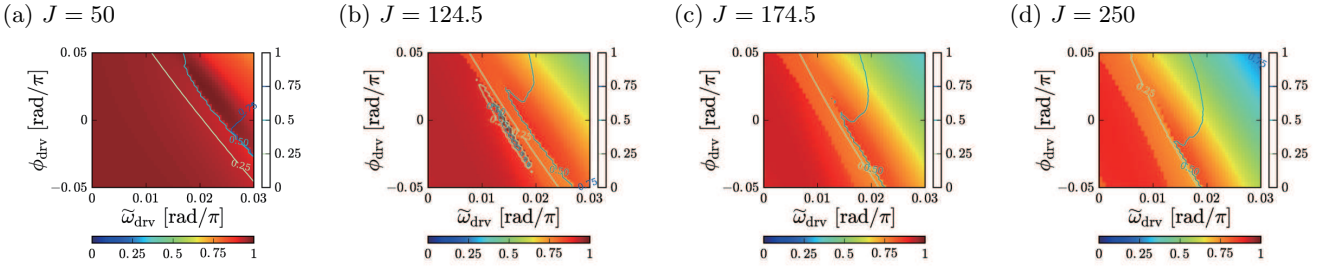

FIG. 3. Contour plots of the fidelity $F_{\rm MSS}(J)$ and the displacement angle $\delta_{\rm MSS}(J)$ [π^{-1}] with respect to the rescaled driving frequency $\tilde{\omega}_{\rm drv}$ and the phase of the driving frequency $\phi_{\rm drv}$ for $J =$ (a) 50, (b) 124.5, (c) 174.5, and (d) 250. The color and the curves indicate the fidelity and the displacement angle, respectively.

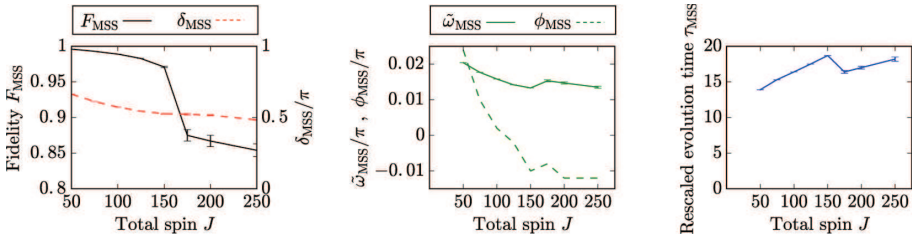

FIG. 4. Total spin dependences of (a) the fidelity and the displacement angle, (b) the set of the rescaled driving frequency and the driving phase, and (c) the rescaled evolution time. (a) The black sold curve with the left scale and the red dotted curve with the right scale represent the fidelity and the displacement angle, respectively. (b) The green solid curve and the green dotted curve indicate the rescaled driving frequency and the driving phase, respectively. In the plots (a), (b), and (c), there are discontinuity between $J = 150$ and 174.5.

contour. This implies that we might be able to further optimise the driving pulse to achieve even high fidelity MSSs.

Finally we evaluate the time to generate a MSS state. To compare the generation time to the typical system coherence time in experiments, we assume the interaction energy of $\chi \sim 3.3$[kHz] for $J = 100$. For this case, the evolution time to achieve a high fidelity MSS can be estimated as 84[μs], which is much smaller than a typical coherence time, 46.5[ms] reported in Ref. [53]. For $J = 200$, assuming the interaction energy of $\chi \sim 0.5$[Hz], we can estimate the evolution time for a state with high fidelity to an MSS to be 85[ms] (< 110[ms] reported in Ref. [45]). The speedup on the MSS generation time can be a significant advantage of this scheme to experimentally generate and test these states. These numbers are promising for relatively large spin ensembles to form a MSS with the current technology.

ACKNOWLEDGMENTS

The authors would thank C. A. Holmes, William J. Munro, Seth Lloyd, Masahito Ueda, Shane Dooley, Michael Hanks, Takeshi Fukuhara, and Nguyen Thanh Phuc. This work is supported by MEXT Grant-in-Aid for Scientific Research on Innovative Areas KAKENHI Grant Number JP15H05870, MEXT Grant-in-Aid for Scientific Research(S) KAKENHI Grant Number JP25220601, and CREST, Japan Science and Technology Agency.

[1] George C. Knee, Kosuke Kakuyanagi, Mao-Chuang Yeh, Yuichiro Matsuzaki, Hiraku Toida, Hiroshi Yamaguchi, Shiro Saito, Anthony J. Leggett, and William J. Munro, Nature Comm, **7**, 13253 (2016).
[2] Horace P. Yuen, Phys. Rev. A **13**, pp. 2226-2243 (1976).
[3] Hwang Lee, Pieter Kok, and Jonathan P. Dowling, J. Mod. Opt. **49**, pp. 2325-2338 (2002); Jonathan P. Dowling, Contemporary Phys. **49**, pp. 125-143 (2008).
[4] Klaus Mølmer and Anders Sørensen, Phys. Rev. Lett. **82**, pp. 1835-1838 (1999); Andres Sørensen and Klaus Mølmer, Phys. Rev. A **62**, 022311 (2000).
[5] G. J. Milburn, arXiv:9908037 [quant-ph] (1999).
[6] D. D. Bhaktavatsala Rao, Nir. Bar-Gill, and Gershon Kurizki, Phys. Rev. Lett. **106**, 010404 (2011).
[7] N. David Mermin, Phys. Rev. Lett. **8**, pp. 1838-1840 (1990).
[8] J. J. Bollinger, Wayne M. Itano, D. J. Wineland, D. J. Heizen, Phys. Rev. A **54**, pp. R4649-R4652 (1996).
[9] Christopher C. Gerry and Rainer Grobe, J. Mod. Opt. **44**, pp. 44-53 (1997).

[10] S. F. Huelga, C. Macchiavello, T. Pellizzari, A. K. Ekert, M. B. Plenio, and J. I. Cirac, Phys. Rev. Lett. **79**, pp. 3865-3868 (1997).

[11] Agedi N. Boto, Pieter Kok, Daniel S. Abrams, Samuel L. Braunstein, Colin P. Williams, and Jonathan P. Dowling, Phys. Rev. Lett. **85** pp. 2733-2736 (2000).

[12] M. W. Mitchell, J. S. Lundeen, and A. M. Steinberg, Nature **429**, pp. 161-164 (2004).

[13] D. Leibfried, M. D. Barrett, T. Schaetz, J. Britton, J. Chiaverini, W. M. Itano, J. D. Jost, C. Langer, D. J. Wineland, Science **304**, pp. 1476-1478 (2004)

[14] Vittorio Giovannetti, Seth Lloyd, Lorenzo Maccone, Science **306**, pp. 1330-1336 (2004).

[15] Luca Pezzé and Augusto Smerzi, Phys. Rev. Lett. **106**, 100401 (2009).

[16] Jonathan A. Jones, Steven D. Karlen, Joseph Fitzsimons, Arzhang Ardavan, Simon C. Benjamin, G. Andrew D. Briggs, John J. L. Morton, Science **324**, pp. 1166-1168 (2009); Stephanie Simmons, Jonathan A. Jones, Steven D. Karlen, Arzhang Ardavan, and John J. L. Morton, Phys. Rev. A **82**, 022330 (2010).

[17] Robert McConnell, Hao Zhang, Senka Ćuk, Jiazhong Hu, Monika H. Schleier-Smith, and Vladan Vuletić, Phys. Rev. A **88**, 063802 (2013).

[18] T. C. Ralph, A. Gilchrist, G. J. Milburn, W. J. Munro, and S. Glancy, Phys. Rev. A **68**, 042319 (2003).

[19] Sean D Barrett, Peter P Rohde, and Thomas M Stace, New J. Phys. **12** 093032 (2010).

[20] Petr Marek and Jaromír Fiurášek, Phys. Rev. A **82**, 014304 (2010).

[21] L.-M. Duan, M. D. Lukin, J. I. Cirac, and P. Zoller, Nature **414**, pp. 413-418 (2001).

[22] F. T. Arecchi, Eric Courtens, Robert Gilmore, and Harry Thomas, Phys. Rev. A **6**, pp. 2211-2237 (1972).

[23] G. S. Agarwal, R. R. Puri, and R. P. Singh, Phys. Rev. A **56**, pp. 2249-2254 (1997).

[24] Sergey M. Chumakov, Alejandro Frank, and Kurt Bernardo Wolf, Phys. Rev. A **60**, pp. 1817-1823 (1999).

[25] Jan Benhelm, Gerhard Kirchmair, Christian F. Roos, and Rainer Blatt, Nature Phys. **4** pp. 463-466 (2008).

[26] A. Voje, J. M. Kinaret, and A. Isacsson, Phys. Rev. B **85** 205415 (2012).

[27] Tomáš Opatrný and Kalus Mølmer, Phys. Rev. A **86** 023845 (2012).

[28] Shane Dooley and Timothy P. Spiller, Phys. Rev. A **90** 012320 (2014).

[29] Hon Wai Lau, Zachary Dutton, Tian Wang, and Christoph Simon, Phys. Rev. Lett. **113** 090401 (2014).

[30] Christopher C. Gerry and Rainer Grobe, Phys. Rev. A **56**, pp. 2390-2396 (1997); *ibid.* **57**, pp. 2247-2250 (1998).

[31] José Recamier, Octavio Castanõs, Rocio Jáuregui and Alejandro Frank, Phys. Rev. A **61** 063808 (2000).

[32] S. D. Bennett, N. Y. Yao, J. Otterbach, P. Zoller, P. Rabl, and M. D. Lukin, Phys. Rev. Lett. **110**, 156402 (2013).

[33] Shane Dooley, Emi Yukawa, Yuichiro Matsuzaki, George C. Knee, William J. Munro, and Kae Nemoto, New J. Phys. **18**, 053011 (2016).

[34] Wei-Bo Gao, Chao-Yang Lu, Xing-Can Yao, Ping Xu, Otfried Gühne, Alexander Goebel, Yu-Ao Chen, Cheng-Zhi Peng, Zeng-Bing Chen, and Jian-Wei Pan, Nature Phys. **6**, pp. 331-335 (2010).

[35] Pieter Kok, Hwang Lee, and Jonathan P. Dowling, Phys. Rev. A **65**, 052104 (2002).

[36] Anne E. Nielsen and Klaus Mølmer, Phys. Rev. A **75**, 063803 (2007).

[37] Yu-Ao Chen, Xiao-Hui Bao, Zhen-Sheng Yuan, Shuai Chen, Bo Zhao, and Jian-Wei Pan, Phys. Rev. Lett. **104**, 043601 (2010).

[38] Ryotaro Inoue, Shin-Ichi-Ro Tanaka, Ryo Namiki, Takahiro Sagawa, and Yoshiro Takahashi, Phys. Rev. Lett. **110**, 163602 (2013).

[39] Navin Khaneja, Roger Brockett, and Steffen J. Glaser, Phys. Rev. A **63**, 032308 (2001); Navin Khaneja and Steffen J. Glaser, Chem. Phys. **267**, pp. 11-23 (2001).

[40] Jun Zhang, Jiri Vala, Shankar Sastry, and K. Birgitta Whaley, Phys. Rev. A **67**, 042313 (2003); Jun Zhang and K. Birgitta Whaley, Phys. Rev. A **71**, 052317 (2005).

[41] M. Kitagawa and M. Ueda, Phys. Rev. A **47**, pp. 5138-5143 (1993).

[42] J. Estève, C. Gross, A. Weller, S. Giovanazzi, and M. K. Oberthaler, Nature **455**, pp. 1216-1219 (2008); C. Gross, T. Zibold, E. Nicklas, J. Estève, and M. K. Oberthaler, Nature **464**, pp. 1165-1169 (2010).

[43] Ian D. Leroux, Monika H. Schleier-Smith, and Vladan Vuletić, Phys. Rev. Lett. **104**, 073602 (2010); Monika H. Schleier-Smith, Ian D. Leroux, and Vladan Vuletić, Phys. Rev. A **81**, 021804(R) (2010).

[44] Max F. Riedel, Pascal Böhi, Yun Li, Theodor W. Hänsch, Alice Sinatra and Philipp Treutlein, Nature **464**, pp. 1170-1173 (2010).

[45] Helmut Strobel, Wolfgang Muessel, Daniel Linnemann, Tilman Zibold, David B. Hume, Luca Pezzè, Augusto Smerzi, and Markus K. Oberthaler, Science **345**, pp. 424-427 (2014).

[46] C. A. Sackett, D. Kielpinski, B. E. King, C. Langer, V. Meyer, C. J. Myatt, M. Rowe, Q. A. Turchette, W. M. Itano, D. J. Wineland and C. Monroe, Nature **404**, pp. 256-259 (2000); D. Leibfried, E. Knill, S. Seidelin, J. Britton, R. B. Blakestad, J. Chiaverini, D. B. Hume, W. M. Itano, J. D. Jost, C. Langer, R. Ozeri, R. Reichle and D. J. Wineland, Nature **438**, pp. 639-642 (2005).

[47] Thomas Monz, Philipp Schindler, Julio T. Barreiro, Michael Chwalla, Daniel Nigg, William A. Coish, Maximilian Harlander, Wolfgang Hänsel, Markus Hennrich, and Rainer Blatt, Phys. Rev. Lett. **106**, 130506 (2011).

[48] Yun Li, P. Treutlein, J. Reichel, and A. Sinatra, Eur. Phys. J. B **68**, pp. 365-381 (2009).

[49] J. I. Cirac, M. Lewenstein, K. Mo?lmer, and P. Zoller, Phys. Rev. A **57**, pp. 1208-1218 (1998).

[50] D. Gordon and C. M. Savage, Phys. Rev. A **59**, pp. 4623-4629 (1999).

[51] A. Micheli, D. Jaksch, J. I. Cirac, and P. Zoller, Phys. Rev. A **67**, 013607 (2003).

[52] H. J. Lipkin, N. Meshkov, and J. Glick, Nucl. Phys. **62**, pp. 188-198 (1965).

[53] Justin G. Bohnet, Brian C. Sawyer, Joseph W. Britton, Michael L. Wall, Ana Maria Rey, Michael Foss-Feig, and John J. Bollinger, Science **352**, pp. 1297-1301 (2016).

[54] S. Chaudhury, A. Smith, B. E. Anderson, S. Ghose, and P. S. Jessen, Nature **461**, pp. 768-771 (2009).

[55] `https://docs.scipy.org/doc/scipy/reference/generated/scipy.`